ENVIRONMENTAL RESEARCH
LETTERS

LETTER • OPEN ACCESS

Increased harvested carbon of cropland in China

ENVIRONMENTAL RESEARCH
LETTERS

OPEN ACCESS

RECEIVED
28 September 2023

REVISED
28 February 2024

ACCEPTED FOR PUBLICATION
5 April 2024

PUBLISHED
23 April 2024

LETTER

Increased harvested carbon of cropland in China

Peiyang Ren[1], Daju Wang[1], Xiaosheng Xia[1], Xiuzhi Chen[1], Zhangcai Qin[1], Jing Wei[1], Shuguang Liu[2], Mike O'Sullivan[3] and Wenping Yuan[4,*]

[1] School of Atmospheric Sciences, Guangdong Province Data Center of Terrestrial and Marine Ecosystems Carbon Cycle, Sun Yat-sen University, Zhuhai, Guangdong 510245, People's Republic of China
[2] National Engineering Laboratory for Applied Technology of Forestry & Ecology in South China, College of Life Science and Technology, Central South University of Forestry and Technology, Changsha 410004, People's Republic of China
[3] Faculty of Environment, Science and Economy, University of Exeter, Exeter EX4 4PY, United Kingdom
[4] Institute of Carbon Neutrality, Sino-French Institute for Earth System Science, College of Urban and Environmental Sciences, Peking University, Beijing 100091, People's Republic of China
[*] Author to whom any correspondence should be addressed.

E-mail: yuanwp3@mail.sysu.edu.cn

Keywords: harvested carbon, cropland, terrestrial ecosystem models, carbon cycle

Supplementary material for this article is available online

Abstract

Crop harvested carbon (HC) is one of the most important components of the carbon cycle in cropland ecosystems, with a significant impact on the carbon budget of croplands. China is one of the most important crop producers, however, it is still unknown on the spatial and temporal variations of HC. This study collected statistical data on crop production at the province and county levels in China for all ten crop types from 1981 to 2020 and analyzed the magnitude and long-term trend of harvested crop carbon. Our results found a substantial increase of HC in cropland from 0.185 Gt C yr^{-1} in 1981 to 0.423 Gt C yr^{-1} in 2020 at a rate of 0.006 Gt C yr^{-1}. The results also highlighted that the average annual carbon sink removal from crop harvesting in China from 1981 to 2020 was 0.32 Gt C yr^{-1}, which was comparable to the net carbon sink of the entire terrestrial ecosystems in China. This study further generated a gridded dataset of HC from 2001 to 2019 in China by using jointly the statistical crop production and distribution maps of cropland. In addition, a model-data comparison was carried out using the dataset and results from seven state-of-the-art terrestrial ecosystem models, revealing substantial disparities in HC simulations in China compared to the dataset generated in the study. This study emphasized the increased importance of HC for estimating cropland carbon budget, and the produced dataset is expected to contribute to carbon budget estimation for cropland ecosystems and the entire China.

1. Introduction

As one of the most important terrestrial ecosystems, cropland plays a crucial role in regulating the terrestrial carbon cycle (Bondeau *et al* 2007). Globally, approximately 12% of the ice-free land surface is occupied by cropland, with large spatio-temporal variations influenced by factors such as population changes, crop product prices, and socio-economic factors (Yuan *et al* 2018). The vegetation gross primary productivity of croplands contributes to 12%–16% of global vegetation gross primary productivity (Cai *et al* 2014), and also partly controls the seasonal fluctuations of the terrestrial carbon cycle (Zeng *et al* 2014). Previous studies have also emphasized the positive relationship between the growth of cropland production and the seasonal variations in atmospheric CO_2 concentration (Gray *et al* 2014). Furthermore, over the past few decades, there has been a notable expansion of cropland at the expense of forests, grasslands, and other ecosystems (Winkler *et al* 2021), leading to an increased contribution to the global carbon cycle (Erb *et al* 2017). Consequently, it is imperative to accurately estimate the magnitude and changes in the carbon cycle for agricultural land areas (Osborne *et al* 2010).

In crop ecosystems, during harvest and removal from cropland, the carbon in grains will be emitted to the atmosphere in a short period along with human and livestock consumption. It is widely acknowledged that the carbon derived from harvested grain significantly influences the carbon budget of the cropland ecosystem (Smith *et al* 2010). Measurements of eddy covariance in 17 European cropland ecosystems showed that the cropland transitioned from carbon sink to carbon source after accounting for harvested carbon (HC) at crop harvest (Moors *et al* 2010). Regional studies also highlighted that HC dominates the carbon budget not only for cropland but also at the entire country level (Ciais *et al* 2010). A recent study estimated that annual carbon losses from cropland harvesting were 0.44 Gt C yr^{-1} within the continental United States, which was 2.56 times of annual mean net carbon sink (0.17 Gt C yr^{-1}) (Liu *et al* 2020). According to statistical yield datasets, the average crop harvest in 25 European countries was 275 and 239 g C m^{-2} yr^{-1} during the period 1990–1999, representing approximately 40% of net vegetation production (Ciais *et al* 2010). The global cropland harvest in 2000 was 3.2 Gt C yr^{-1}, which is around half of the total biomass harvest or the global terrestrial net carbon sink (Wirsenius 2003, Krausmann *et al* 2008, Friedlingstein *et al* 2022).

The carbon harvested significantly affects the carbon budget of cropland ecosystems, and it has been the most common land management-related process considered in current terrestrial ecosystem models (Gervois *et al* 2004, Lokupitiya *et al* 2009, Drewniak *et al* 2013, Pongratz *et al* 2018). To integrate agriculture into a comprehensive land biosphere model, Kucharik and Brye (2003) incorporated a crop growth model (i.e. Erosion-Productivity Impact Calculator) into the Integrated BIosphere Simulator (IBIS) (Foley *et al* 1996, Yuan *et al* 2014) to simulate the agricultural process. More recently, the community Land Model Version 5 (CLM5.0) introduced a crop module to accurately represent crop distributions and management, including dynamic major crop distributions, fertilization, and irrigation management (Lombardozzi *et al* 2020).

Although previous research has made valuable efforts, there is still great uncertainty in accurately quantifying harvested carbon in cropland (HCC) ecosystems (Smith *et al* 2010, Lun *et al* 2016). For example, the CLM5.0 crop model can reproduce the observed long-term trend of crop yields with relative accuracy before 1990 but showed a substantial underestimation after 1990 (Lombardozzi *et al* 2020). There are still numerous challenges for terrestrial ecosystem models to simulate crop yield. Specifically, models need accurately represented the multiple crop properties (e.g. planting density, crop variety, crop breeding), field management practices (e.g. irrigation, tillage, fertilization), and impacts of climate change (e.g. drought, flood, heatwave), which largely affect crop yield and crop-carbon cycle interactions (Yuan *et al* 2016). Most of the above factors highly depend on human decisions and activities, which strongly challenge the model's ability (Cheng *et al* 2014). Few terrestrial ecosystem models, therefore, can represent crop properties and management practices due to the complicated interactions between human decisions and biogeochemical cycle processes (Zhang *et al* 2018). Therefore, many models used the globally fixed ratio of removed carbon with large uncertainties in simulating regional and global carbon budgets (Stocker *et al* 2011, Malyshev *et al* 2015). In contrast, a large volume of statistical data is more readily available, which provides a good opportunity to generate a dataset of HC instead of relying on terrestrial ecosystem models (National Bureau of Statistics of China 2020).

As one of the largest crop producers globally, China contributes approximately 610 million tons of grain annually, representing 20% of the total global crop production (FAO 2021). In addition, the cropland accounts for about 13% of total land area in China (Chen *et al* 2022b), and plays an important role in determining terrestrial carbon budget. However, it is still unknown about the magnitude and trend of HC in China due to limited information and insufficient model capability. This study first collected agricultural census data at the province and county levels from 1981 to 2020 and investigate the magnitude and long-term trend of harvested crop carbon. In addition, we generated a gridded dataset of harvested crop carbon from 2001 to 2019 based on the existing crop distribution maps in China. Finally, based on this newly produced gridded dataset, we examined the model performance of seven state-of-the-art terrestrial ecosystem models in reproducing harvested crop carbon.

2. Data and method

2.1. Agricultural statistical data

This study collected province and county-level statistical data on the planting area, yield, and production of various crops from agricultural yearbooks of various regions (National Bureau of Statistics of China 2020). We collected province-level statistical data of 10 crop types for all investigated 31 provinces from 1981 to 2020, which was used to analyze the long-term trend of harvested crop carbon in China. To generate the gridded dataset of harvested crop carbon, i.e. Terrestrial Ecosystem Disturbance-HCC (TED-HCC), we collected county-level statistical data of crop production from 2001 to 2019 to match with the distribution map of cropland (see section S2). Province-level data was obtained from the agricultural section of the National Statistical Yearbooks, and county-level crop production data was sourced from the sections on key economic indicators of counties (cities, districts) in the statistical yearbooks of each province. For the county without statistical production through the period of 2001–2019, we conducted a gap-filling method to fill the missing county-level statistical production. (1) For a given

Table 1. Carbon content of 10 crop types.

Type	Content (%)	Type	Content (%)
Grain	0.5	Sugar beet	0.05
Oilseeds	0.57	Tea	0.5
Cotton	0.56	Tobacco	0.5
Hemp	0.438	Fruit	0.05
Sugarcane	0.438	Vegetable	0.026

Data from Baes *et al* (1984).

county, the missing statistical production was less than three years continuously, then a linear equation was used to fill the missing statistical production based on the statistics of the adjacent two years. (2) If the years of missing statistical production were more than three years continuously, the mean ratio between county-level and province-level statistical production in the other years was calculated, and calculated the statistical production of this given year for this given county based on the mean ratio and province-level production of this year.

2.2. Estimation of harvested crop carbon

Harvested crop carbon was estimated by considering crop production data from provincial or county statistical sources. Given the significant variations in carbon content among different crops, this study employed specific carbon content values of each crop (table 1) (Baes *et al* 1984) to calculate the HC based on their statistical production. The investigated crops include ten types: grain (wheat, corn, and rice), oilseeds, cotton, hemp, sugar beet, sugarcane, tea, tobacco, fruit, and vegetables.

Furthermore, we allocated county-level HC of 10 crops to the pixel level in each county, with a focus on wheat, maize, and rice, which are key for determining harvested crop carbon and account for 74% of China's total crop production. Using the ChinaCropArea1km dataset, we assigned county-level HC to corresponding 1×1 km pixels for these grains. This method, assuming higher HC in pixels with greater leaf area index, applies an equation (see section S2) to calculate the allocated HC at each pixel. For crops like sugarcane and oilseeds without specific distribution maps, we used the China Land Cover Dataset for allocation, after removing areas of wheat, maize, and rice. Due to the absence of comprehensive crop distribution maps and to reduce uncertainties, the gridded datasets were aggregated into a 10×10 km resolution for comparison with ecosystem model simulations of HC.

2.3. Generation of gridded HC dataset and model comparison

To examine the performance of state-of-the-art terrestrial ecosystem models in reproducing the spatial and temporal variations of harvested crop carbon, this study generated a gridded dataset of HCC ecosystems from 2001 to 2019, referred to as TED-HCC, as a component of the TED dataset. The gridded dataset was generated through the combined utilization of statistical data, crop distribution datasets, and satellite-based vegetation index. The detailed method of generating gridded HC dataset was introduced in the supplementary (see section S1).

This study collected simulations of harvested crop carbon from the Global Carbon Budget (Friedlingstein *et al* 2022). Although there were 17 ecosystem models in Global Carbon Budget, 7 terrestrial ecosystem models provided the output of harvested crop carbon: the Community Land Model (CLM5.0; Lawrence *et al* 2019), Integrated BIosphere Simulator (IBIS; Yuan *et al* 2014), Interaction Sol-Biosphère-Atmosphère Model (ISBA; Noilhan and Mahfouf 1996), the land component of the MPI Earth System Model (JSBACH; Reick *et al* 2021), Lund–Potsdam–Jena General Ecosystem Simulator model (LPJ-GUESS; Sitch *et al* 2003), a newly developed version of the terrestrial biosphere model (OCN; Zaehle and Friend 2010), and the Organizing Carbon and Hydrology In Dynamic Ecosystems (ORCHIDEE; Krinner *et al* 2005). To meticulously analyze interannual variations, we employed linear detrending on the HC outputs from each terrestrial ecosystem model. This method meticulously subtracted the calculated linear trend from the original data series, enabling us to isolate and focus on the cyclical fluctuations inherent in the data.

3. Results

3.1. Magnitude of HC and its spatial-temporal changes

Based on the province-level statistical data, we first analyzed the magnitude of HC and its spatiotemporal patterns. During the past 40 years, the mean HC of the cropland ecosystem in China was determined to be 0.32 Gt C yr^{-1} in China (figure 1). The HC in China showed substantial temporal change during the past 40 years. Specifically, total HC increased by about 2.3 times, from 0.185 Gt C yr^{-1} in 1981 to 0.423 Gt C yr^{-1} in 2020 (figure 1). All crop types showed an increasing trend, with grain types (i.e. rice, wheat, and maize) contributing the most to China's total harvested growth (68.3%) (figure 2(b)) because of their larger share (figure 2(a)).

Notably, there were significant variations in the distribution of HC across different crop types. The grain, including maize, rice, and winter wheat, accounted for the largest proportion of total HC at 75.9% through 1981–2020 (figure 2(a)). In addition, sugarcane, vegetables, and oilseeds contributed shares of 11.1%, 5.2%, and 4.3% respectively. Collectively, these four crop types accounted for

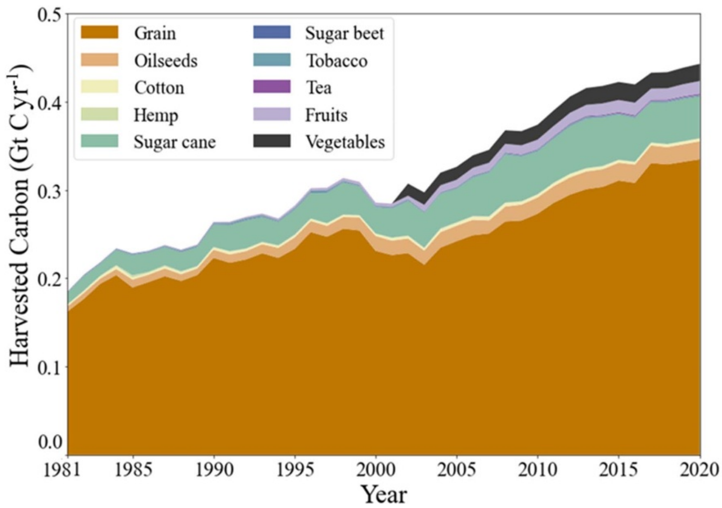

Figure 1. Long-term changes of harvested carbon in cropland ecosystem in China.

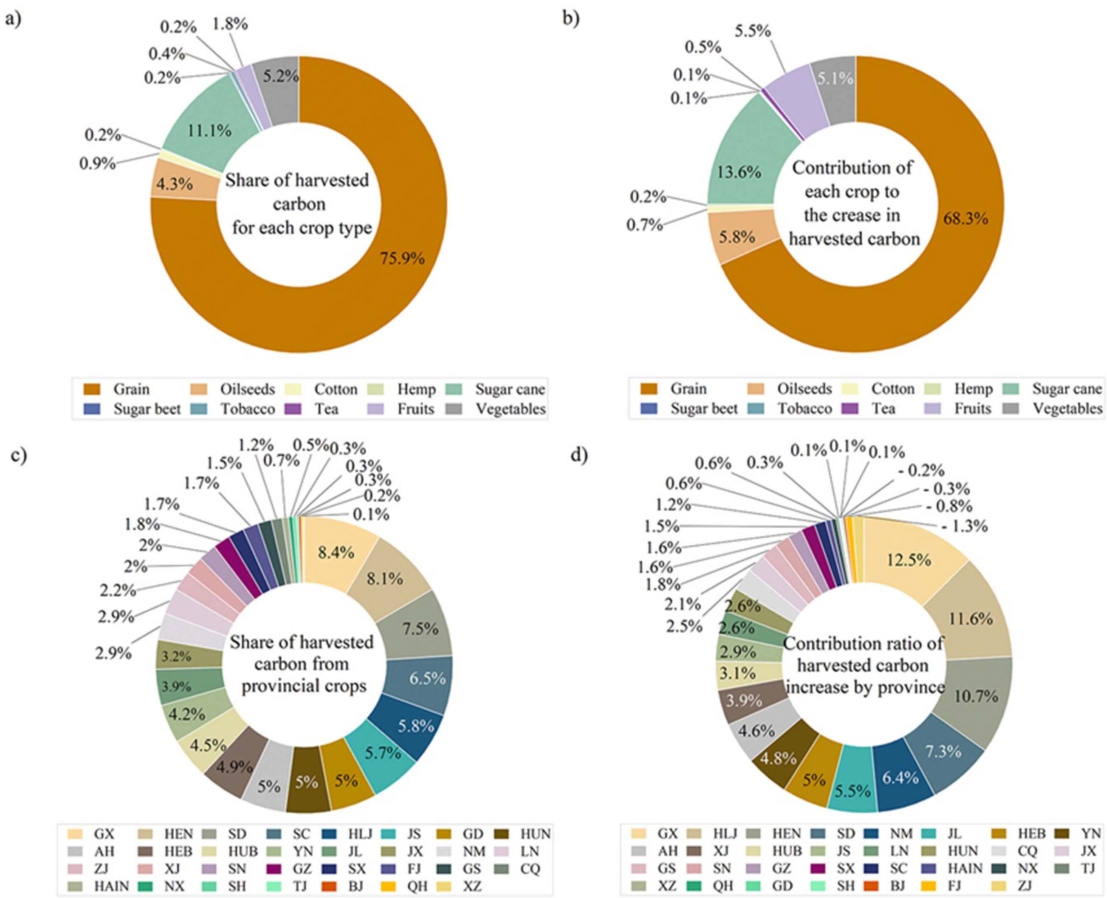

Figure 2. Percentage share of various crops in harvested carbon and contribution to long-term changes in China. (a) Share of various crops to the total harvested carbon. (b) Share of various crops to long-term changes of harvested carbon. (c), (d) are similar to (a), (b) but indicate provincial shares, and the abbreviations indicate the province (figure S1).

more than 96% of the total HC (figure 2(a)). Other six types of crops (i.e. cotton, hemp, sugar beet, tobacco, tea, and fruits) only shared 3.7% of the total HC (figure 2(a)). Of these, hemp, tobacco and tea accounted for the smallest share, all at 0.2%. Large differences of harvested crop carbon also were found among the various provinces. The largest five provinces, i.e. Guangxi, Henan, Shandong, Sichuan, and Heilongjiang, contributed more than 36% of total HC in China (figures 2(c) and S1). While, these

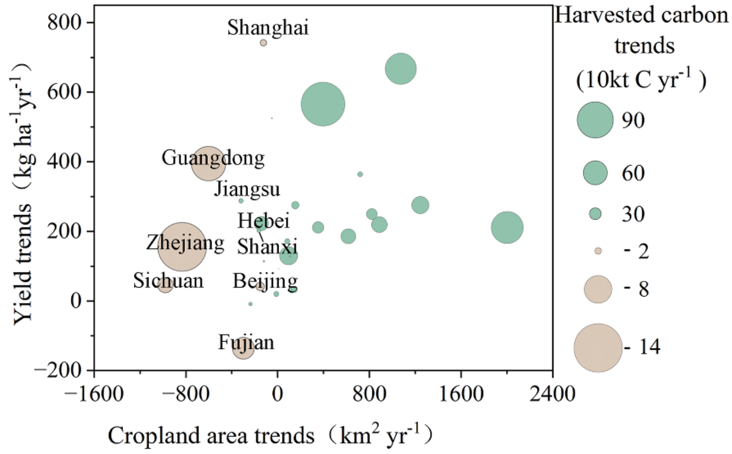

Figure 3. The relationship between the change trends of the total planting area of all crops in each province of China from 1981 to 2020, the change trends of crop yield, and the change trends of crop production, where the horizontal axis represents the area, the vertical axis represents the yield, and the size of the circle represents the change trends of harvested carbon.

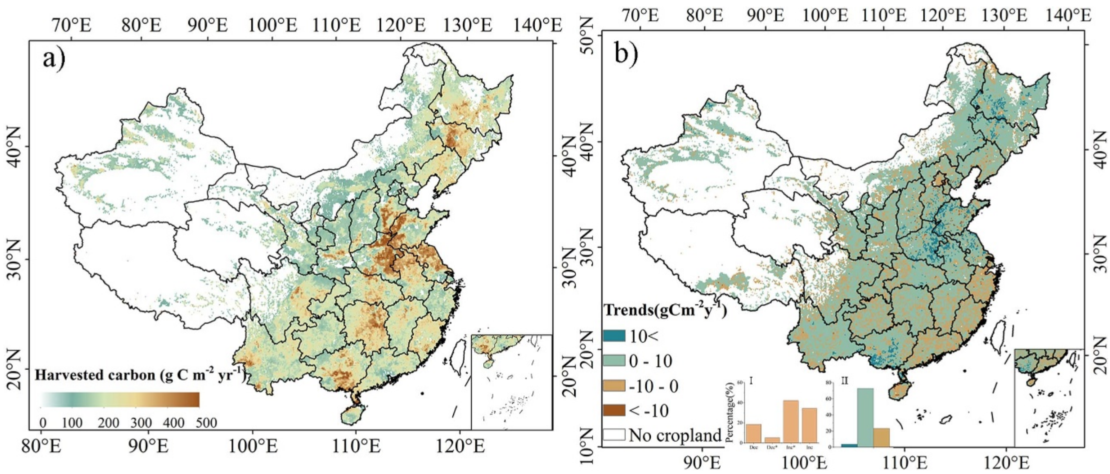

Figure 4. Intensity (a) and trend (b) of harvested crop carbon from 2001 to 2019. The small bar chart I on the lower left corner of panel b shows the proportion of four situations: significantly decreased ($p < 0.05$), insignificantly decreased, insignificantly increased and significantly increased. The bar chart II displays the distribution of grid point trends in >10, 0–10, −10–0, and <−10 g C m^{-2} yr^{-1}.

five provinces also contributed the largest increased shares, and contributed more than 48.5% increases of HC in China (figure 2(d)).

Both planting area and yields have had a significant impact on harvested crop carbon over the past 40 years (figure 3). Most provinces increased in planting area and yields, which jointly promoted an increase in crop HC. Only a few provinces, such as Zhejiang, Guangdong, Fujian, Beijing, Shanghai, Sichuan, showed a decline in HC in the last 40 years (figure 3). As figure 3 shown, only Fujian province, the decreased HC was attributed to the decreases of both planted area and yield (figure 3), and other 5 mainly due to a decrease in planted area (figure 3). There were several provinces with decreased planting areas, but the HC still showed the increased trend, e.g. Shanxi, Jiangsu (figure 3).

3.2. Gridded dataset of HC

Based on the statistical dataset, this study generated a gridded dataset of HC in China with a spatial resolution of 10 × 10 km (i.e. TED-HCC dataset). Notably, the dataset excludes Hongkong, Macau, and Taiwan due to the lack of statistical data. Figure 4 reveals that the HC was mainly distributed in Northeast, North, and Southwest China. The intensity of HC varies from 1 g C m^{-2} yr^{-1} to 467 g C m^{-2} yr^{-1} (as depicted in figure 4(a)). Through the past two decades (2001–2019), the intensity of HC showed an increasing trend over more than 42.1% of regions (34.4% with a significant upward trend), and only 18.4% showed a decreased trend (5.1% with a significant downward trend) (figure 4(b)). It should be noticed that the decreasing trend mainly occurred in the Southeast region.

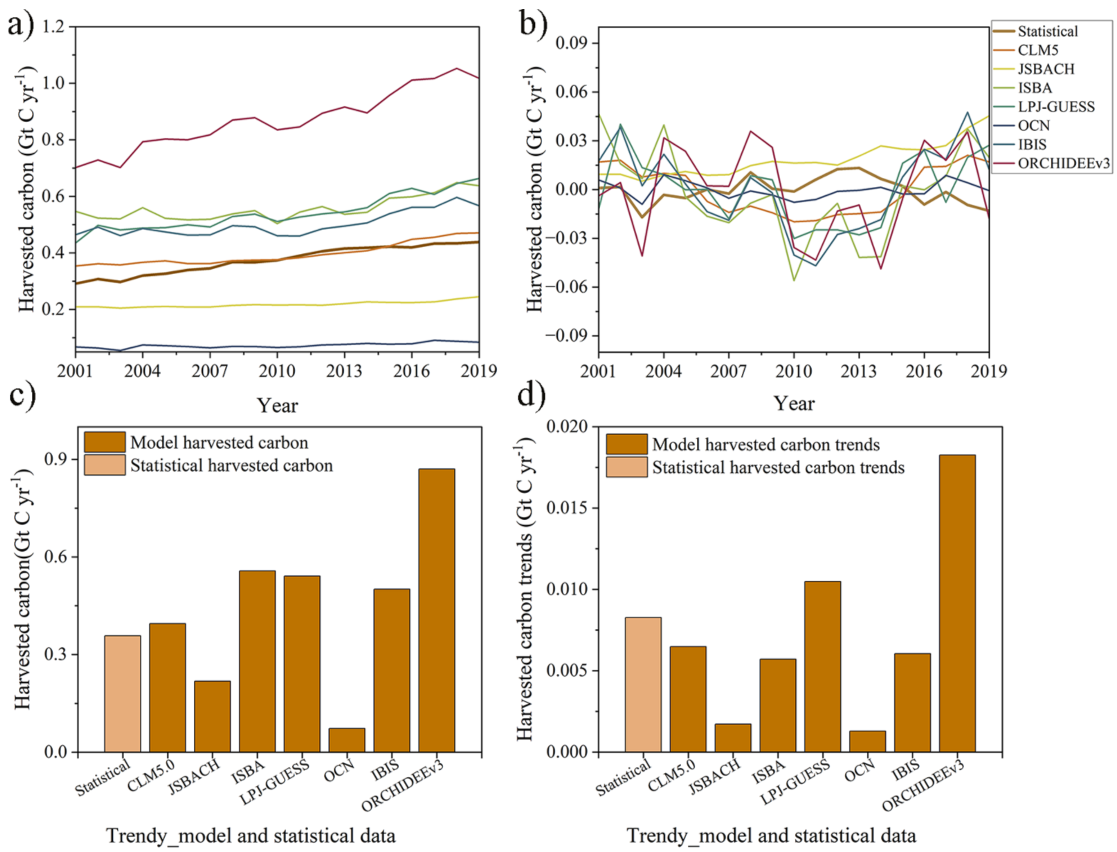

Figure 5. Comparison between harvested carbon derived from statistical data and simulations of seven models. (a) The temporal variations of harvested carbon; (b) the detrended temporal variations of harvested carbon; (c) the harvested carbon averaged through 2001–2019, (d) the harvested carbon trends averaged through 2001–2019.

It should be noticed that the availability of statistical crop production highly determined the accuracy of TED-HCC dataset. Although there existed data gaps of county-level crop production, the statistics of major crops were available. Grain crops (maize, wheat, and rice) contributed the largest share (75.9%) of total HC (figure 2(a)), and the collected county-level statistical production accounted for 68% provincial production averaged from 2001 to 2019 (figure S2(a)). The sugarcane and oilseed were the second and fourth largest contributors of the total HC (i.e. 11.1% and 4.3%), and the county-level statistical production accounted for 76% of the provincial statistical production. Therefore, these three crops accounted for more than 90% of HC, and the available county-level statistical production accounted for 72% of provincial production.

3.3. Model-data comparison

Based on the TED-HCC dataset of HC generated by this study, we further evaluated the model performance of seven terrestrial ecosystem models for simulating HC. On average, the simulated HC by seven models ranged from 0.14 Gt C yr^{-1} to 0.87 Gt C yr^{-1} through 2001–2019, and there were 10.4% to 143.2% differences compared with the HC derived from statistical data (0.36 Gt C yr^{-1}) (figure 5(c)). The mean simulations by CLM5.0 (0.39 Gt C yr^{-1}) (figure 5(c)) were quite close to HC derived from statistical data. However, the simulations by other six models showed the large differences with HC derived from statistical data (figure 5(c)). The simulated HC trends by seven models ranged from 0.0012 Gt C yr^{-1} to 0.018 Gt C yr^{-1} 2001–2019, with CLM5.0 still demonstrating the trend closest to the statistical results (figure 5(d)), while the trends simulated by the other six models continue to exhibit significant differences from the statistical data. Furthermore, although there is a substantial variation in the inter-annual changes of the six models compared to the statistical data, a closer inspection reveals that the trends of ISBA, ORCHIDEE, and IBIS models are quite similar to each other, as depicted in figures 5(a) and (b).

Our results also revealed significant variations in the spatial distribution of simulated HC among seven terrestrial ecosystem models when compared to the HC derived from the TED-HCC dataset (figures 6 and S3). The majority of models can characterize the main spatial pattern with the large intensity of HC

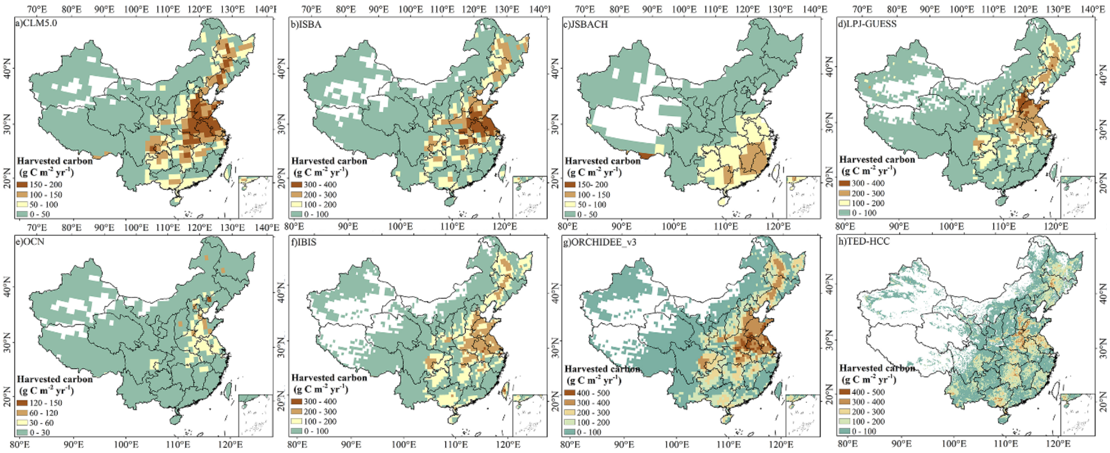

Figure 6. The mean intensity of harvested carbon derived from seven terrestrial ecosystem models from 2001 to 2019. Figures (a)–(g) show the simulations of seven models, and (i) shows the harvested carbon derived from the TED-HCC dataset.

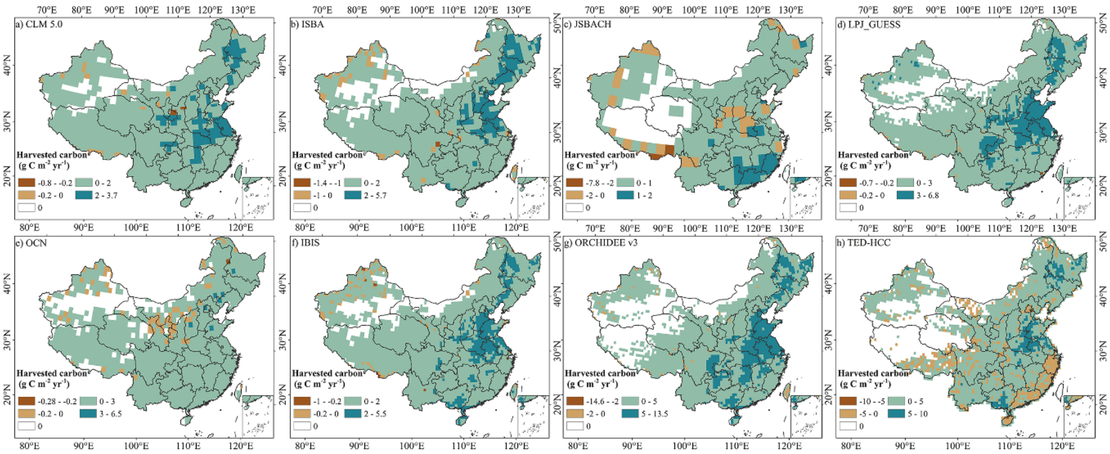

Figure 7. Long-term trends in harvested carbon from 2001 to 2019 simulated by seven process-based ecosystem models. Figures (a)–(g) show the simulations of seven models, and (h) shows the harvested carbon trends derived from the TED-HCC dataset.

in Northeast, North, Southeast, and Southwest China (figure 6). However, several models (e.g. JSBACH and OCN) failed to accurately depict the spatial distribution compared with the gridded dataset generated by this study (figures 6(c) and (e)). For example, the JSBACH model only showed Southeast China as the main region of HC in China and lost other regions such as Northeast China (figure 6(c)). While most models demonstrated a significant intensity of HC in North China, the most substantial variations among models were also observed in this region (figure 6).

We further analyzed the model performance for reproducing the trend of HC compared with the observed trend. In general, seven ecosystem models showed large spatial differences in the simulated trends (figures 7 and S4). CLM5.0, ISBA, LPJ-GUESS, IBIS, and ORCHIDEE showed a similar spatial pattern on the trend of simulated HC, and a largely increased trend was observed in northern China (figures 7(a), (b), (d), (f) and (g)). However, the spatial pattern showed large differences from the observed trend in the TED-HCC dataset, and large increases were found in Northeast China, and decreased trends existed in Southern China (figure 7(h)). Although the other two models showed the decreased trend of HC over some regions (figures 7(c) and (e)), the decreased regions largely differed with the TED-HCC dataset (figure 7(h)). In addition, the observed HC shows significantly increased trend from 2001 to 2019 with a rate of 0.0083 Gt C yr^{-1} (figure 5(d)).

4. Discussion

Harvested crop carbon play an important role in determining carbon budget of cropland and even entire terrestrial ecosystems in China. According to our dataset, there were 0.32 Gt C yr^{-1} exported from cropland ecosystem to human society averaged from 1981 to 2020, which was comparable with the terrestrial carbon sink in China (i.e. 0.19–0.26 Gt C yr^{-1}) (Piao *et al* 2009). More important, the HC substantially increased by the rate of 0.006 Gt C yr^{-1} through the past 40 years, from 0.18 Gt C yr^{-1} in 1981 to 0.42 Gt C yr^{-1} in 2020 (figure 1). This trend is closely linked to the observed increase in crop yield benefit (tech-enhanced harvest index, climate-induced multi-cropping), as higher yields directly translate to greater amounts of harvested crop carbon. As HC is one of the largest carbon fluxes in cropland ecosystems, the increased HC substantially impacts carbon budget. Based on eddy covariance measurements of rotation cropland in the North China Plain, a study estimated a winter wheat ecosystem to be a large carbon sink (359 g C m^{-2} yr^{-1}), but only a carbon sink of 90 g C m^{-2} yr^{-1} after accounting for HC (Wang *et al* 2015). In addition, numerous studies highlighted the harvest index (the ratio of grain to aboveground biomass) largely increased (Yang and Zhang 2010), which implied more aboveground biomass allocated to grain and reduced the magnitude of straw resulting in less accumulation of soil organic carbon in cropland ecosystems.

Although the total harvested crop carbon highly increases over the entire China during the past 40 years, there are large spatial heterogeneity of changes in HC. In general, the harvested crop carbon showed the increased trend in the north China, but decreased trend in south China. Previous study supported our conclusion and showed substantial regional shifts in crop cultivation and the subsequent impacts on crop production in China (Yuan *et al* 2018). They found that South China have lost large planting areas of cropland in order to pursue industry and commerce, but Northeast and Northwest China have witnessed increases in planting areas (Yuan *et al* 2018). The competition for resources between agricultural and nonagricultural sectors and across regions has been intensified by the rapid industrialization, urbanization, strong income growth, and population expansion.

Model-data comparison conducted in this study showed the large uncertainties of state-of-the-art terrestrial ecosystem models for simulating HC (figures 5–7, S3 and S4). Figure S5 showed the provincial crop areas derived from LUH2 dataset was close to the statistical areas at most provinces, and which implied the model capability was the more important reason for the uncertainties of simulated HC. Simulating harvested crop carbon is a considerable challenge for terrestrial ecosystem models (Lombardozzi *et al* 2020). The primary difficulty arises from the need to accurately represent crop management at regional and global scales (Licker *et al* 2010). Substantial efforts have been made to produce regional and global maps of cropland management (Xiang *et al* 2020). However, there are still large uncertainties due to the lack of statistical and survey datasets (Siebert *et al* 2010). For example, a recent study found that the widely used FAO irrigation dataset (i.e. Global Map of Irrigation Areas) in China (Xiang *et al* 2019) has low accuracy. In addition, several other important factors highly determined crop yield, but there was no regional and global information yet (Cabas *et al* 2010). Previous studies highlighted the improvement of crop variety contributed substantially to the rising of crop yield (Xiong *et al* 2014). A recent study showed that satellite-based light use efficiency incorporating regional information on crop variety can significantly improve the estimates of crop yield (Dong *et al* 2020). However, spatial information on crop variety was lacking in most regions. Therefore, most process-based terrestrial ecosystem models did not integrate several important crop management information (Pongratz *et al* 2018), which led to large uncertainties in simulating crop production.

TED-HCC, therefore, has an important implication for carbon budget estimates as the HC largely determined the carbon budget of cropland ecosystems (Zhang *et al* 2015). Therefore, a national dataset of HC generated by this study had an important role in improving the estimates of country and global-level carbon budgets. Currently, Global Carbon Budget provided several important forest and cropland disturbance information, which were difficult to simulate by terrestrial ecosystem models (Friedlingstein *et al* 2022). For example, the LUH2 dataset provided gridded annual harvest forest carbon (Chini *et al* 2021), which was quite similar to harvest carbon in the cropland ecosystems in terms of strong human decision. However, Global Carbon Budget did not provide harvest crop carbon due to data scarcity (Friedlingstein *et al* 2022). Our results showed the averaged harvested crop carbon in China is 0.32 Gt C yr^{-1} from 1981 to 2020, which is larger than the harvested forest carbon reported by the LUH2 dataset in China (0.04 Gt C yr^{-1} averaged from 1981 to 2020). More importantly, the former will emit into the atmosphere at a faster rate compared with harvested forest carbon. In addition, this dataset (i.e. TED-HCC) is urgently needed for the top-down method (i.e. atmospheric inverse model) to deduct HC. As an important carbon budget assessment method, atmospheric inverse models have been widely used to estimate the regional and global terrestrial carbon sink (Chen *et al* 2022a). It should be noticed that atmospheric inverse models estimated carbon flux between land and atmosphere, but did not simulate the process of crop harvest, and the carbon fixed in the crop grain will not be removed from cropland. Therefore, atmospheric inverse models may overestimate the carbon sink in the cropland because they did not simulate the emission of harvested crop carbon.

5. Conclusion

HC, a crucial component of the carbon budget in cropland ecosystems, poses a well-documented challenge for terrestrial ecosystem models. This study collected statistical production of 10 crop types from 1981 to 2020 and calculated the HC with crop harvest. The results showed that the total HC increased about 2.3 times during the past 40 years, from 0.18 Gt C yr^{-1} in the1981 to 0.42 Gt C yr^{-1} in 2020. The grain-type crop (i.e. rice, wheat, and maize) makes the largest contribution (68.3%) to total increases of HC in China. In addition, based on the statistical crop production data, this study generated the gridded dataset of HC (TEC-HCC, i.e. Terrestrial Ecosystem Disturbance-Harvested Carbon in Cropland Ecosystems) over entire China (did not include Hongkong, Macau, and Taiwan) jointly using crop distribution maps and satellite-based vegetation index. The spatial resolution of this dataset is 10 km × 10 km. Based on this newly produced dataset, and we evaluated the performance of the seven terrestrial ecosystem models for simulating HC in China. Several models could reproduce the spatial patterns of HC, but all models failed to reproduce the temporal variations during the past 40 years. This study highlighted a substantial increased trend of harvested crop carbon during the past 40 years, and the produced dataset has a large potential for estimating the national carbon budget and to be a benchmark of state-of-the-art terrestrial ecosystem models.

Data availability statements

Any data that support the findings of this study are included within the article and/or the supplementary materials.

The harvested carbon dataset of cropland in China from this study is available at: https://doi.org/10.6084/m9.figshare.22785800.v4 (Ren *et al* 2023).

The dataset consists of a single NetCDF file containing agricultural annual harvested carbon images, with each image representing the carbon harvested per square meter of each grid cell for a specific year (unit: g C m^{-2} yr^{-1}). To obtain the total carbon harvested for each grid cell, please multiply the carbon harvested value in each image file by the corresponding grid cell area.

Acknowledgments

This work was financially supported by the key project of the National Natural Science Foundation of China (42141020).

Conflict of interest

The authors declare that they have no conflict of interest.

ORCID iDs

Daju Wang https://orcid.org/0000-0003-4645-8589
Xiaosheng Xia https://orcid.org/0000-0002-3847-0521
Zhangcai Qin https://orcid.org/0000-0001-9414-4854
Mike O'Sullivan https://orcid.org/0000-0002-6278-3392

References

Baes I I I, Sharp R D, Sjoreen A L and Shor R W 1984 *Review and analysis of parameters for assessing transport of environmentally released radionuclides through agriculture* (Oak Ridge National Lab. (ORNL)) (available at: www.osti.gov/biblio/6355677)

Bondeau A *et al* 2007 Modelling the role of agriculture for the 20th century global terrestrial carbon balance *Glob. Change Biol.* **13** 679–706

Cabas J, Weersink A and Olale E 2010 Crop yield response to economic, site and climatic variables *Clim. Change* **101** 599–616

Cai W, Yuan W, Liang S, Zhang X, Dong W, Xia J, Fu Y, Chen Y, Liu D and Zhang Q 2014 Improved estimations of gross primary production using satellite-derived photosynthetically active radiation *J. Geophys. Res. Biogeosci.* **119** 110–23

Chen B, Chen F, Ciais P, Zhang H, Lü H, Wang T, Chevallier F, Liu Z, Yuan W and Peters W 2022a Challenges to achieve carbon neutrality of China by 2060: status and perspectives *Sci. Bull.* **67** 2030–5

Chen X, Yu L, Du Z, Liu Z, Qi Y, Liu T and Gong P 2022b Toward sustainable land use in China: a perspective on China's national land surveys *Land Use Policy* **123** 106428

Cheng K, Ogle S M, Parton W J and Pan G 2014 Simulating greenhouse gas mitigation potentials for Chinese croplands using the DAYCENT ecosystem model *Glob. Change Biol.* **20** 948–62

Chini L *et al* 2021 *Land-use harmonization datasets for annual global carbon budgets* Antroposphere—Land Cover and Land Use (available at: https://essd.copernicus.org/preprints/essd-2020-388/essd-2020-388.pdf)

Ciais P *et al* 2010 The European carbon balance. Part 2: croplands *Glob. Change Biol.* **16** 1409–28

Dong J, Fu Y, Wang J, Tian H, Fu S, Niu Z, Han W, Zheng Y, Huang J and Yuan W 2020 Early-season mapping of winter wheat in China based on Landsat and Sentinel images *Earth Syst. Sci. Data* **12** 3081–95

Drewniak B, Song J, Prell J, Kotamarthi V R and Jacob R 2013 Modeling agriculture in the community land model *Geosci. Model Dev.* **6** 495–515

Erb K-H *et al* 2017 Land management: data availability and process understanding for global change studies *Glob. Change Biol.* **23** 512–33

FAO 2021 World food and agriculture—statistical yearbook 2021 FAO (available at: www.fao.org/documents/card/en/c/cb4477en)

Foley J A, Prentice I C, Ramankutty N, Levis S, Pollard D, Sitch S and Haxeltine A 1996 An integrated biosphere model of land surface processes, terrestrial carbon balance, and vegetation dynamics *Glob. Biogeochem. Cycles* **10** 603–28

Friedlingstein P *et al* 2022 Global carbon budget 2021 *Earth Syst. Sci. Data* **14** 1917–2005 (available at: https://essd.copernicus.org/articles/14/1917/2022/)

Gervois S, de Noblet-ducoudré N, Viovy N, Ciais P, Brisson N N, Seguin B and Perrier A 2004 Including croplands in a global biosphere model: methodology and evaluation at specific sites *Earth Interact.* **8** 16

Gray J M, Frolking S, Kort E A, Ray D K, Kucharik C J, Ramankutty N and Friedl M A 2014 Direct human influence on atmospheric CO_2 seasonality from increased cropland productivity *Nature* **515** 398–401

Krausmann F, Erb K-H, Gingrich S, Lauk C and Haberl H 2008 Global patterns of socioeconomic biomass flows in the year 2000: a comprehensive assessment of supply, consumption and constraints *Ecol. Econ.* **65** 471–87

Krinner G, Viovy N, de Noblet-ducoudré N, Ogée J, Polcher J, Friedlingstein P, Ciais P, Sitch S and Prentice I C 2005 A dynamic global vegetation model for studies of the coupled atmosphere-biosphere system *Glob. Biogeochem. Cycles* **19** 1

Kucharik C J and Brye K R 2003 Integrated biosphere simulator (IBIS) yield and nitrate loss predictions for Wisconsin maize receiving varied amounts of nitrogen fertilizer *J. Environ. Qual.* **32** 247–68

Lawrence D M *et al* 2019 The community land model version 5: description of new features, benchmarking, and impact of forcing uncertainty *J. Adv. Model. Earth Syst.* **11** 4245–87

Licker R, Johnston M, Foley J A, Barford C, Kucharik C J, Monfreda C and Ramankutty N 2010 Mind the gap: how do climate and agricultural management explain the "yield gap" of croplands around the world *Glob. Ecol. Biogeogr.* **19** 769–82

Liu J *et al* 2020 Critical land change information enhances the understanding of carbon balance in the United States *Glob. Change Biol.* **26** 3920–9

Lokupitiya E, Denning S, Paustian K, Baker I, Schaefer K, Verma S, Meyers T, Bernacchi C J, Suyker A and Fischer M 2009 Incorporation of crop phenology in Simple Biosphere Model (SiBcrop) to improve land-atmosphere carbon exchanges from croplands *Biogeosciences* **6** 969–86

Lombardozzi D L, Lu Y, Lawrence P J, Lawrence D M, Swenson S, Oleson K W, Wieder W R and Ainsworth E A 2020 Simulating agriculture in the community land model version 5 *J. Geophys. Res. Biogeosci.* **125** e2019JG005529

Lun F, Canadell J G, He L, Yang B, Liu M, Yuan Z, Tian M, Liu J and Li W 2016 Estimating cropland carbon mitigation potentials in China affected by three improved cropland practices *J. Mt. Sci.* **13** 1840–54

Malyshev S, Shevliakova E, Stouffer R J and Pacala S W 2015 Contrasting local versus regional effects of land-use-change-induced heterogeneity on historical climate: analysis with the GFDL earth system model *J. Clim.* **28** 5448–69

Moors E J *et al* 2010 Variability in carbon exchange of European croplands *Agric. Ecosyst. Environ.* **139** 325–35

National Bureau of Statistics of China 2020 China statistical yearbook Mary Martin (available at: https://books.google.nl/books?id=XSD7zQEACAAJ)

Noilhan J and Mahfouf J-F 1996 The ISBA land surface parameterisation scheme *Glob. Planet. Change* **13** 145–59

Osborne B, Saunders M, Walmsley D, Jones M and Smith P 2010 Key questions and uncertainties associated with the assessment of the cropland greenhouse gas balance *Agric. Ecosyst. Environ.* **139** 293–301

Piao S, Fang J, Ciais P, Peylin P, Huang Y, Sitch S and Wang T 2009 The carbon balance of terrestrial ecosystems in China *Nature* **458** 1009–13

Pongratz J *et al* 2018 Models meet data: challenges and opportunities in implementing land management in Earth system models *Glob. Change Biol.* **24** 1470–87

Reick C H, Gayler V, Goll D, Hagemann S, Heidkamp M, Nabel J E M S, Raddatz T, Roeckner E, Schnur R and Wilkenskjeld S 2021 JSBACH 3—the land component of the MPI earth system model: documentation of version 3.2 (available at: https://pure.mpg.de/pubman/faces/ViewItemOverviewPage.jsp?itemId=item_3279802)

Ren P, Wang D and Xia X 2023 Terrestrial ecosystem disturbance-harvested carbon in cropland (https://doi.org/10.6084/m9.figshare.22785800.v4)

Siebert S, Portmann F and Döll P 2010 Global patterns of cropland use intensity *Remote Sens.* **2** 1625–43

Sitch S *et al* 2003 Evaluation of ecosystem dynamics, plant geography and terrestrial carbon cycling in the LPJ dynamic global vegetation model *Glob. Change Biol.* **9** 161–85

Smith P *et al* 2010 Measurements necessary for assessing the net ecosystem carbon budget of croplands *Agric. Ecosyst. Environ.* **139** 302–15

Stocker B D, Strassmann K and Joos F 2011 Sensitivity of Holocene atmospheric CO_2 and the modern carbon budget to early human land use: analyses with a process-based model *Biogeosciences* **8** 69–88

Wang Y, Hu C, Dong W, Li X, Zhang Y, Qin S and Oenema O 2015 Carbon budget of a winter-wheat and summer-maize rotation cropland in the North China Plain *Agric. Ecosyst. Environ.* **206** 33–45

Winkler K, Fuchs R, Rounsevell M and Herold M 2021 Global land use changes are four times greater than previously estimated *Nat. Commun.* **12** 2501

Wirsenius S 2003 Efficiencies and biomass appropriation of food commodities on global and regional levels *Agric. Syst.* **77** 219–55

Xiang K, Ma M, Liu W, Dong J, Zhu X and Yuan W 2019 Mapping irrigated areas of Northeast China in comparison to natural vegetation *Remote Sens.* **11** 825

Xiang K, Yuan W, Wang L and Deng Y 2020 An LSWI-based method for mapping irrigated areas in China using moderate-resolution satellite data *Remote Sens.* **12** 4181

Xiong W, van der Velde M, Holman I P, Balkovic J, Lin E, Skalský R, Porter C, Jones J, Khabarov N and Obersteiner M 2014 Can climate-smart agriculture reverse the recent slowing of rice yield growth in China? *Agric. Ecosyst. Environ.* **196** 125–36

Yang J and Zhang J 2010 Crop management techniques to enhance harvest index in rice *J. Exp. Bot.* **61** 3177–89

Yuan W *et al* 2014 Multiyear precipitation reduction strongly decreases carbon uptake over Northern China *J. Geophys. Res. Biogeosci.* **119** 881–96

Yuan W *et al* 2016 Severe summer heatwave and drought strongly reduced carbon uptake in Southern China *Sci. Rep.* **6** 18813

Yuan W, Liu S, Liu W, Zhao S, Dong W, Tao F, Chen M and Lin H 2018 Opportunistic market-driven regional shifts of cropping practices reduce food production capacity of China *Earths Future* **6** 634–42

Zaehle S and Friend A D 2010 Carbon and nitrogen cycle dynamics in the O-CN land surface model: 1. Model description, site-scale evaluation, and sensitivity to parameter estimates *Glob. Biogeochem. Cycles* **24** 1

Zeng N, Zhao F, Collatz G J, Kalnay E, Salawitch R J, West T O and Guanter L 2014 Agricultural green revolution as a driver of increasing atmospheric CO_2 seasonal amplitude *Nature* **515** 394–7

Zhang J, Tian H, Yang J and Pan S 2018 Improving representation of crop growth and yield in the dynamic land ecosystem model and its application to China *J. Adv. Model. Earth Syst.* **10** 1680–707

Zhang X, Izaurralde R C, Manowitz D H, Sahajpal R, West T O, Thomson A M, Xu M, Zhao K, LeDuc S D and Williams J R 2015 Regional scale cropland carbon budgets: evaluating a geospatial agricultural modeling system using inventory data *Environ. Model. Softw.* **63** 199–216